Journal of Applied Electrochemistry (2006) 36:195–204
DOI 10.1007/s10800-005-9053-3

Electrochemical behaviour of a magnesium alloy containing rare earth elements

F. ZUCCHI*, V. GRASSI, A. FRIGNANI, C. MONTICELLI and G. TRABANELLI
Corrosion Study Centre "A. Daccò" – Chemistry Department, University of Ferrara, L. Borsari 46, 44100, Ferrara, Italy
*(*author for correspondence, fax: +39 0532 240709, e-mail: zhf@unife.it)*

Received 4 April 2005; accepted in revised form 18 August 2005

Key words: corrosion, electrochemical techniques, rare earths, WE43 magnesium alloy

Abstract

The corrosion of a magnesium alloy containing rare earth elements (WE43 type alloy) was studied in 0.05 and 0.5 M Na_2SO_4 or 0.1 and 1 M NaCl solutions using electrochemical techniques: linear polarization resistance, potentiodynamic polarization, impedance measurements. The electrolytes favoured anodic magnesium oxidation but the presence of rare earth elements improved the tendency of magnesium to passivation. The dissolution rates in chlorides were higher than in sulphates because chlorides, in contrast to sulphates, interfered with the formation and maintenance of a protective layer of corrosion products which decreased the severity of the attack. The effects of galvanic corrosion due to cathodic intermetallic precipitates at grain boundaries were particularly evident in chloride media at long testing times.

1. Introduction

Magnesium alloys are widely used in the automotive, aircraft and aerospace industries and interest in their application is continuously increasing. The most common Mg alloys are those alloyed with Al and Mn (e.g. AM50 and AM60) and with Al and Zn (e.g. AZ91), whose mechanical properties and corrosion behaviour are well established. Other magnesium alloys, which have good castability, high strength at high temperature and good creep resistance, are obtained with rare earth (RE) elements (chiefly WE54 and WE43 alloys) [1, 2].

Data concerning corrosion and electrochemical behaviour of Mg alloys are numerous [3–14], but those concerning Mg-RE alloys are scarce [15–20]. However, the latter data seem to indicate that, in addition to favourable high temperature properties, certain Mg-RE alloys present good corrosion resistance. Unsworth [15] showed that WE54 alloy had a corrosion resistance comparable to that of A356 and A347 Al alloys in 28 day tests in sea water. Geary [16] measured a corrosion rate of 0.4 mm y^{-1} on WE43 in NaCl solution and reported that this alloy had the lowest maximum pit depth of all the Mg alloys tested. Nakatsugawa [17] compared the polarization curves of AZ91D and different Mg-RE alloys, WE54 included, recorded in 5% NaCl solution saturated with $Mg(OH)_2$. The corrosion potentials of Mg-RE alloys were more negative than that of AZ91D, and the anodic curves of Mg-RE were characterized by a very high slope up to -1.65 $V_{/SCE}$, in contrast with AZ91D anodic curve. The authors deduced from the electrochemical impedance spectra that Mg-RE alloys have a corrosion resistance about four times higher than that of AZ91D.

As magnesium alloys suffer from localized corrosion in the presence of a multiphase structure, due to galvanic effects, the formation of less cathodic intermetallic compounds can justify the higher corrosion resistance exhibited by the Mg-RE alloys [18]. The surface oxide enrichment in RE elements may also play a role by producing a more corrosion resistant film [19]. Nakatsugawa [17] assumed that the presence of RE accelerates the kinetics of MgH_2 formation, which works as a barrier against further magnesium dissolution.

In this work the corrosion behaviour of a WE43 type alloy was studied in solutions of moderately or highly aggressive anions (sulphates and chlorides, respectively) by electrochemical techniques.

2. Experimental

All the tests were performed on specimens machined from a cast WE43 type alloy (containing 3.92% Y, 2.09% Nd and 0.48% Zr). The specimens ($30\times20\times3$ mm) for the weight loss tests and the electrodes ($10\times10\times3$ mm) for electrochemical tests were

treated with emery papers up to N. 1000 grade, washed with distilled water, degreased with acetone and immediately tested. The aggressive solutions were not deaerated 0.05 and 0.5 M Na_2SO_4 or 0.1 and 1 M NaCl solutions, at 25 ± 0.1 °C.

The time dependence of the corrosion rate was followed by measuring the polarization resistance (R_p) by linear polarization resistance (LPR) technique. The potential was raised from 10 mV below to 10 mV above the corrosion potential (E_{CORR}), with a scanning rate of 0.1 mV s^{-1}. Anodic and cathodic polarization curves were recorded starting from the corrosion potential, usually after 1 and 24 h immersion in the aggressive solutions, with a potential scanning rate of 0.2 mV s^{-1}.

Electrochemical impedance spectra (EIS) were recorded at E_{CORR}, in the frequency range from 100 kHz to 1 mHz, with a sinusoidal signal perturbation of 10 mV.

All the electrochemical measurements were performed with Advanced Electrochemical System Parstat 2263 by Princeton Applied Research.

The dissolution rates were determined by weight loss measurements in 168 h tests. At the end of the tests the specimens were pickled in CrO_3 + 1% Ag_2CrO_4 boiling solution for 2 min and the dissolution rates (V_{DISS}) were expressed in mdd (mg dm^{-2} day^{-1}).

For comparison purposes, some tests were performed on 99.8 Mg alloy specimens, mainly in the dilute sulphate solution.

3. Results

3.1. *WE structure and attack morphology*

Figure 1 shows the structure of WE43 alloy observed by SEM. A eutectic lamellar structure was evident at the grain boundaries. EDX analysis spectra showed that the eutectic phases (points 2 and 3, spectra 2 and 3) were richer in Y and Nd (e.g. peaks at 2 and 5.3 keV) than the base material (point 4, spectrum 4). The composition of the eutectic lamellae was not uniform: the grey zone (point 3) contained more Nd and other RE than the white zone (point 2). A grain disbonding phenomenon can be induced by the occurrence of an internal galvanic corrosion process, connected to the cathodic intermetallic phases precipitated at grain boundaries [9].

In the series of micrographs of Figure 2, the initial stages of the corrosion attack are displayed: the polished WE43 alloy surface was observed after 0.5; 2; 10 and 35 min immersions in 0.1 M NaCl solution. The corrosion attack began around the eutectic phase and

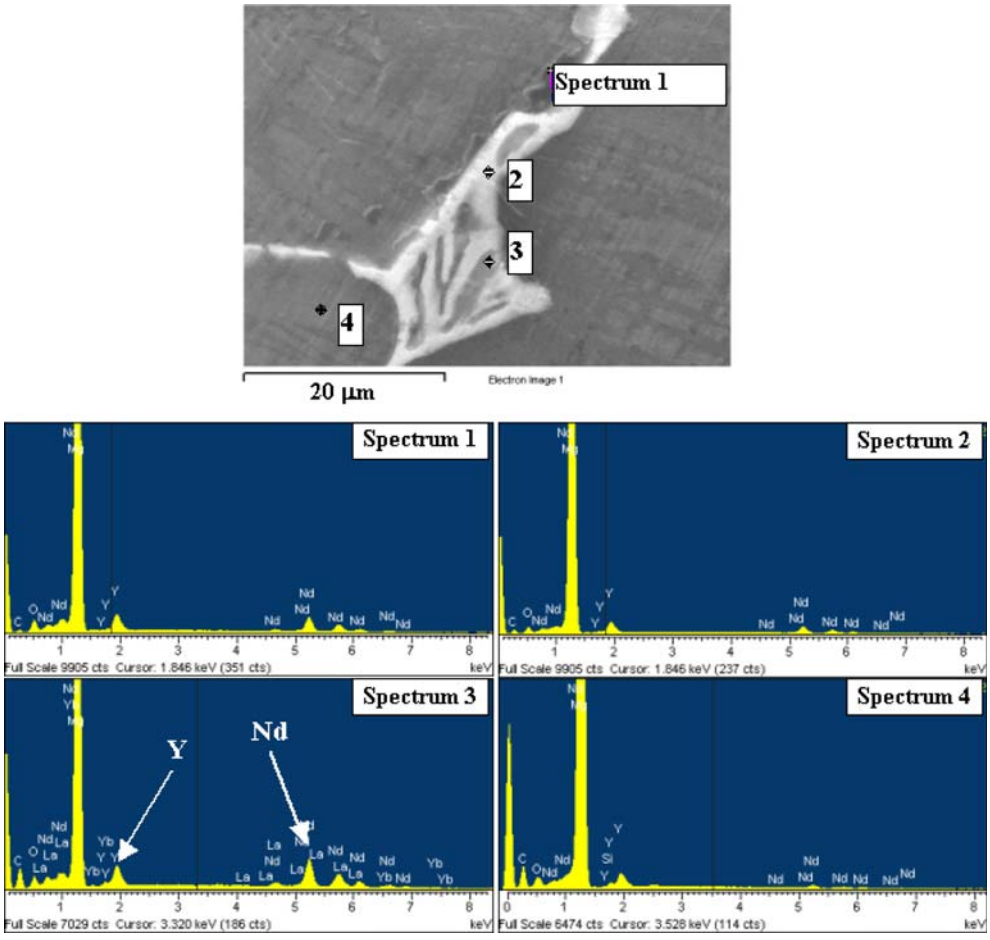

Fig. 1. SEM image and punctual EDX analysis of Mg WE43 alloy.

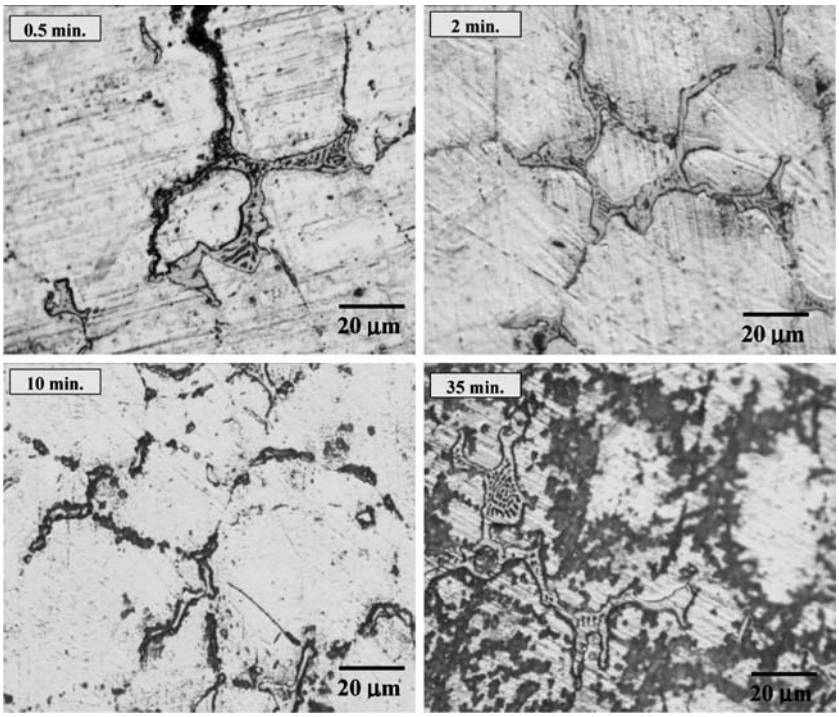

Fig. 2. Micrographs of the first stages of the attack on WE43 alloy.

successively expanded on the grain surface; finally (Figure 3), the α phase grains were preferentially attacked, while the eutectic phase remained unaltered. The heavy undermining of the eutectic phase was found in the concentrated solutions, chiefly in the chloride one; this type of attack was much less evident in the dilute solutions, mainly in the sulphate one (Figure 3). Therefore, the latter environment determined an almost general corrosive attack, while the former a more severe and localized attack.

At the end of the test the specimen surface was covered with a thick layer of corrosion products. Usually the corrosion product film of magnesium alloys presented a multilayered structure [12, 21–25]. For instance, Nordlien et al. observed an inner MgO–$Mg(OH)_2$ cellular layer, a dense thin intermediate MgO region and an outer

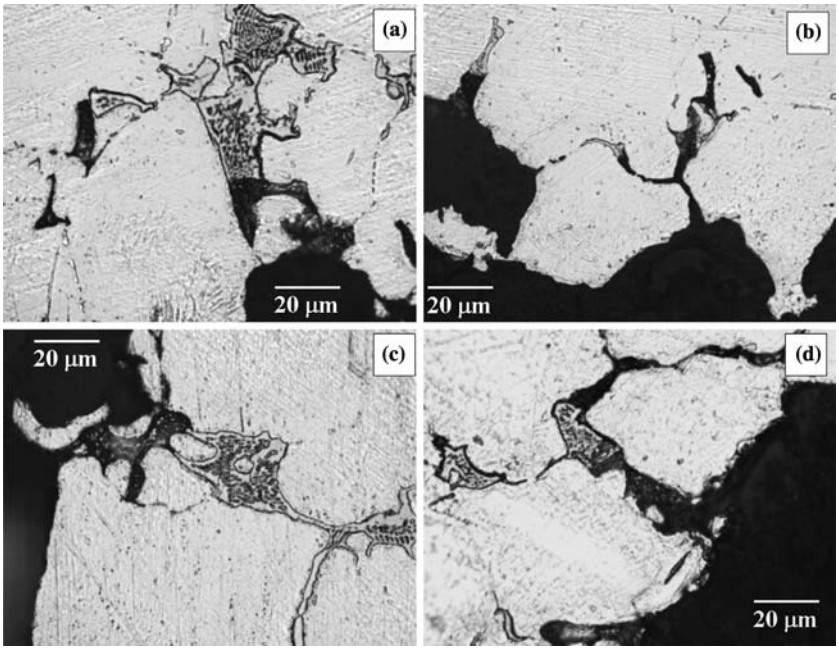

Fig. 3. Micrographs of the section of the specimens corroded for 168 h in the various environments: 0.05 (a) and 0.5 (b) M Na_2SO_4; 0.1 (c) and 1 M (d) NaCl.

thick platelet-like porous layer, rich in magnesium hydroxide, occurring by a dissolution–precipitation mechanism [22–24]; Baril et al. did not find the intermediate layer [25]. The inner layer is reputed to be responsible of the passive behaviour of the alloy, while the intermediate layer to control cation egress and water diffusion.

However, some authors have also postulated the presence of a layer of magnesium hydride, MgH_2 [17].

3.2. *Dissolution rates*

Table 1 collects the dissolution rates (V_{DISS}) of WE43 alloy in dilute and concentrated sodium sulphate and sodium chloride solutions, measured at short (6 h) or long (168 h) immersion times. At short immersion time, the data dispersion was limited (about 15% variation coefficient), while at long immersion time the variation coefficient was about 30%.

In both chlorides and sulphates, and at both immersion times, V_{DISS} increased by augmenting the amount of dissolved salt. In the sulphate solutions, from 6 to 168 h, V_{DISS} reduced to almost one half of the initial value for the formation of a protective layer of magnesium corrosion products (which, at the end of the tests, was eliminated by the pickling procedure). Such a protective layer was unable to form or last in the chloride solutions, particularly in the concentrated one: at low chloride content, V_{DISS} was not linked to the immersion time, whereas at high chloride content, V_{DISS} shifted from 224 to 341 mdd by increasing the testing time. Therefore, after 6 h, chlorides were slightly more aggressive than sulphates, but after 168 h these differences in the dissolution rates were much more evident.

In the case of 99.8 Mg alloy, the dissolution rates reached a value of 193 mdd after 120 h immersion in 0.05 M Na_2SO_4, i.e. 99.8 Mg alloy corroded about four-fold faster than the alloy containing RE elements.

In every case, during these tests, the solution pH shifted from an initial value close to 6 to an almost constant value close to 10 after 60 min of immersion.

3.3. *Linear polarization resistance*

Figure 4 shows the R_p values of WE43 electrodes determined in the different solutions. In diluted sulphate and chloride solutions R_p rapidly increased during the first 16–20 h of immersion (i.e. the corrosion rate decreased), then it slowly increased or remained constant till the end of the test. In the concentrated sulphate solution, R_p increased up to 3.5 kΩ cm^2, during the initial 2 h of immersion, then it underwent a quick decrease, down to 1.2 kΩ cm^2 after 12 h. Finally, at the end of the test, R_p attained a value of 0.4 kΩ cm^2. In concentrated chloride solution, R_p initially augmented as in the diluted solution, but after about 10 h, when it attained a value close to 2 kΩ cm^2, a sudden decrease to around 0.3 kΩ cm^2 was observed; successively R_p swung around this low value.

In dilute media, the continuous decrease in the corrosion rate with time evidenced the formation of a more or less protective layer of corrosion products, which was more effective in the sulphate solution. In contrast, in concentrated solutions, after some hours, a degradation of this layer took place. The attained constant R_p value indicated the achievement of an equilibrium between passivating film formation and dissolution. The lower R_p values in the concentrated chloride media did agree with the higher tendency of these anions to damage the passive layer.

Table 1. Dissolution rates of WE43 and 99.8 Mg alloys from weight losses

Alloy	Electrolyte	Conc./M	V_{DISS}/mdd	
			6 h	168 h
WE43	NaCl	0.1	115	95
		1	224	341
	Na_2SO_4	0.05	91	45
		0.5	176	101
99.8 Mg	Na_2SO_4	0.05	–	193*

*120 h testing.

3.4. *Polarization curves*

Figure 5 collects the polarization curves of WE43 type alloy recorded in the sulphate solutions at different testing times. The anodic polarization curves were assumed to represent the oxidation of magnesium to mono-valent Mg^+ ion [10, 20], while the cathodic ones represented the cathodic hydrogen evolution through water reduction; both reactions developed more easily on film-free areas. Furthermore, hydrogen evolution could also take place through the direct reaction between water and dissolved mono-valent Mg^+ ions [10, 20].

At short immersion times, the anodic polarization currents were favoured by a high sulphate concentration and, after 1 h immersion, E_{CORR} was -1.8 V_{SCE} in the dilute solution and -1.85 V_{SCE} in the concentrated one. In both environments, the anodic curve initially presented a high slope, characteristic of a passive film behaviour. In the concentrated solution, this slope markedly decreased at an anodic overvoltage of about 300 mV; in the dilute solution no abrupt slope change was evident up to -1.3 V_{SCE}. By prolonging the immersion time, the build-up of a protective surface film induced a decrease in the anodic polarization currents and, consequently, an ennoblement of E_{CORR}, which, after 24 h, attained a value close to -1.7 V_{SCE} in both solutions. A high anodic slope was again measured, up to an anodic polarization of about 200 mV. At this immersion time, the cathodic polarization currents of hydrogen evolution were slightly stimulated compared to those measured after 1 h immersion, most likely as a result of the increase in the corroded area. However, these curves were not affected by the sulphate concentration. At even longer testing times (96 h), the

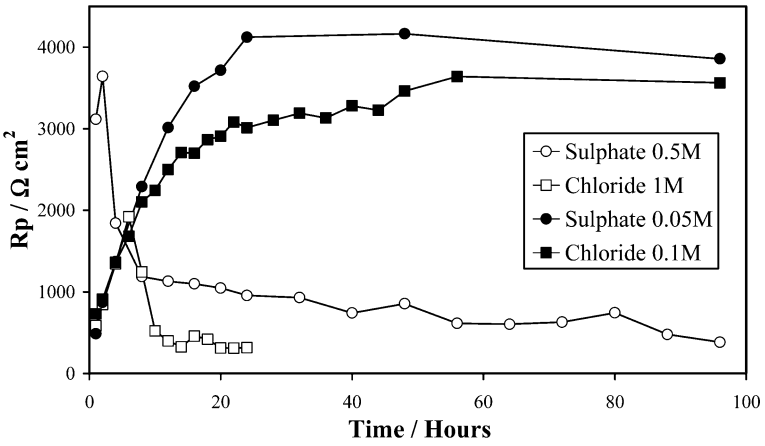

Fig. 4. R_p vs time recorded on WE43 electrodes in diluted and concentrated Na_2SO_4 or NaCl solutions.

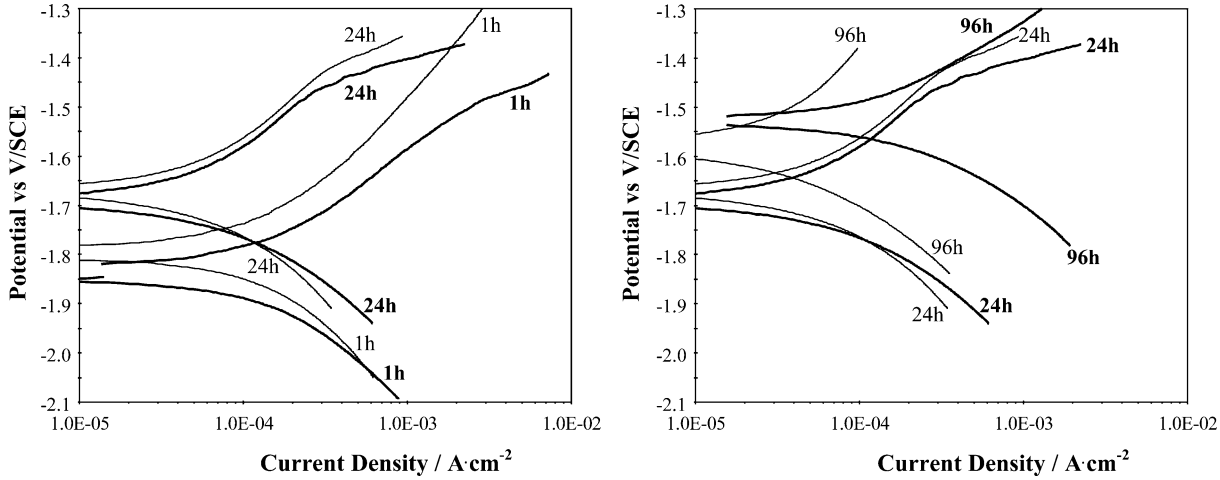

Fig. 5. Polarization curves recorded on WE43 electrodes at different immersion times in dilute (thin lines) or concentrated (thick lines) Na_2SO_4 solutions.

above-mentioned positive effects, due to the build-up of a protective surface film, were only observed in the dilute solution, while in the concentrated one the marked increase in the cathodic polarization currents suggested an enlargement in the corroded area or a reduction in the protective characteristics of the passivating film.

Figure 6 compares the polarization curves of 99.8 Mg with those of the alloy containing RE elements, after 24 h immersion in the sulphate solutions. Owing to its high impurity content which particularly stimulates HER [13], 99.8 Mg displayed higher cathodic polarization currents than those recorded on the latter alloy. Consequently E_{CORR} values of 99.8 Mg alloy were more positive than those of WE43 alloy. The anodic polarization curves clearly showed that the presence of RE elements improved the magnesium capability to passivate, because lower polarization currents and a wider potential range with high anodic overvoltage were found on WE43 alloy, compared to 99.8 Mg. The figure also shows that such a tendency to the formation of a protective surface film was also evident in the more concentrated solution.

In 0.1 M NaCl the anodic curve of WE43 alloy showed two slopes, but the potential range with the high slope was narrower than in the previous solution (Figure 7). Also in this case, at longer immersion times, lower anodic polarization currents were recorded, which induced a marked E_{CORR} ennoblement, that was, however, more limited than that detected in the sulphate solution. In 1 M NaCl a very narrow high-slope region was still present in the anodic polarization curve after 1 h immersion, but it almost disappeared after 24 h. In this case the diminution in the anodic polarization currents at longer immersion times were much lower than those found in the sulphate solution.

The stimulation of the anodic polarization currents for WE43 alloy, due to the electrolyte concentration, was more evident in chloride media than in sulphate solutions, even at long immersion times, but again the cathodic reaction was not affected by the anion concentration.

A comparison between the polarization curves of WE43 recorded in chloride and sulphate solutions after 24 h immersion (Figure 8) clearly showed that the cathodic polarization curves were independent of the

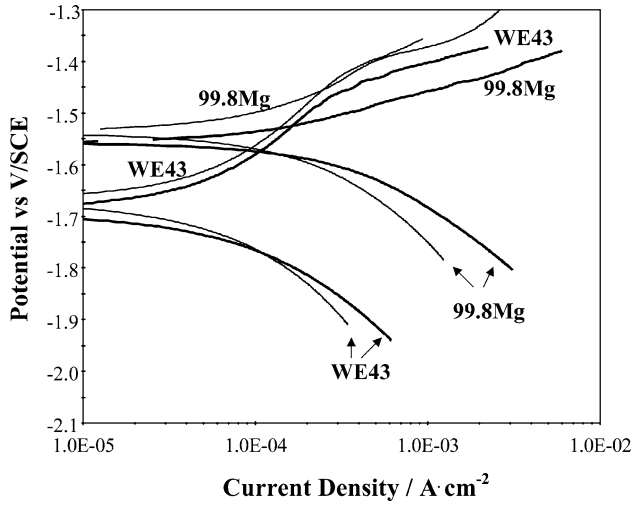

Fig. 6. Polarization curves recorded on WE43 and 99.8 Mg electrodes after 24 h of immersion in dilute (thin lines) or concentrated (thick lines) Na_2SO_4 solutions.

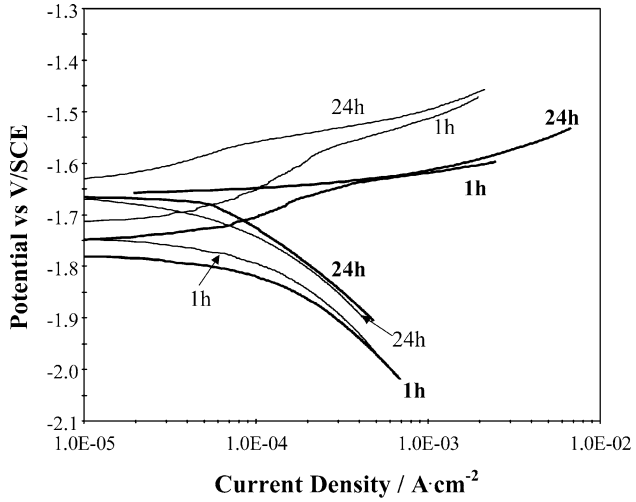

Fig. 7. Polarization curves recorded on WE43 electrodes after 1 and 24 h of immersion in dilute (thin lines) or concentrated (thick lines) NaCl solutions.

anion type, but chlorides, which interfered with the formation or preservation of a protective surface film [4], particularly at elevated concentrations, markedly increased magnesium anodic oxidation.

3.5. *EIS measurements*

As in the case of pure Mg and Mg alloys [5–8, 17], EIS spectra of WE43 alloy were characterized by two, scarcely depressed, capacitive semicircles, followed by the beginning of an inductive loop at frequencies lower than 0.1 Hz. Their dimensions depended on the type and concentration of the electrolyte and on the testing time (Figure 9). For instance, in dilute sulphates, the high frequency (*hf*) semicircle enlarged continuously in the first 24 h immersion, then it remained constant; a rather similar trend was found in dilute chlorides. In the former environment, the medium frequency (*mf*) semicircle, scarcely defined on immersion, increased similarly to the *hf* one. In the latter solution, it enlarged only during the first 8 h immersion, and then some fluctuations were recorded. In general, in the concentrated solutions, after some time from the immersion, the *hf* and *mf* loops tended to decrease.

The *hf* semicircle has been assigned to charge transfer and film effects, the *mf* semicircle to relaxation of mass transport through the corrosion product layer and, finally, the low frequency (*lf*) inductive loop has been connected to relaxation of adsorbed species, such as $Mg(OH)^{+}_{ads}$ or $Mg(OH)_2$ [5, 7, 8].

As previously proposed for pure magnesium [5, 7, 8], the *hf* response of WE43 alloy can be fitted by an equivalent circuit (EC) made up of a series of two R–C parallel combinations: one, a charge transfer resistance (R_{CT}) in parallel with a double layer capacitance (C_{DL}), the other, a resistance related to the film of corrosion products (R_F) in parallel to its capacitance (C_F). It has been ascertained that the resistance associated with *hf* loop can be used to determine magnesium alloy corrosion rate [5, 6].

Although a different analysis of magnesium alloy impedance spectra can be proposed [12, 10], the present analysis was preferred because it takes into consideration the limitations that the presence of a corrosion product layer exerts on the corrosion process [5, 7, 8].

The trend of the charge transfer resistance of WE43 in sulphates was similar to that in chlorides, both in dilute and concentrated solutions (Figure 10). In dilute media, R_{CT} values were almost equal in both environments: R_{CT} almost doubled in the first day of immersion, from about 25–30 to 60 Ω cm^2, then it remained more or less constant. In concentrated media, R_{CT} values, lower than those recorded in the dilute ones, increased for a much

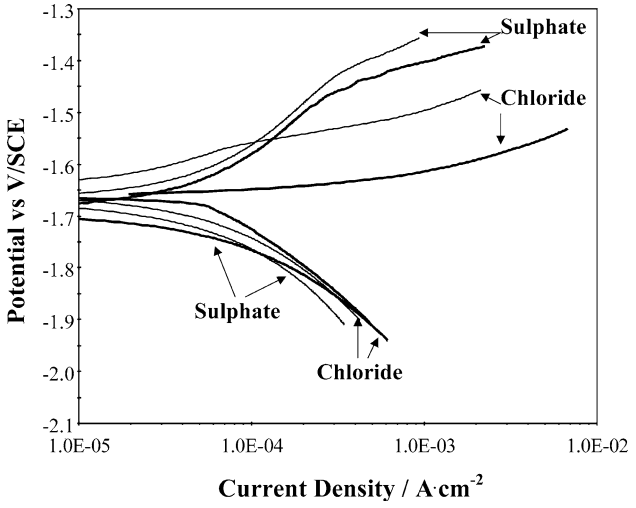

Fig. 8. Anodic and cathodic polarization curves recorded in dilute (thin lines) or concentrated (thick lines) Na_2SO_4 or NaCl solutions after 24 h immersion.

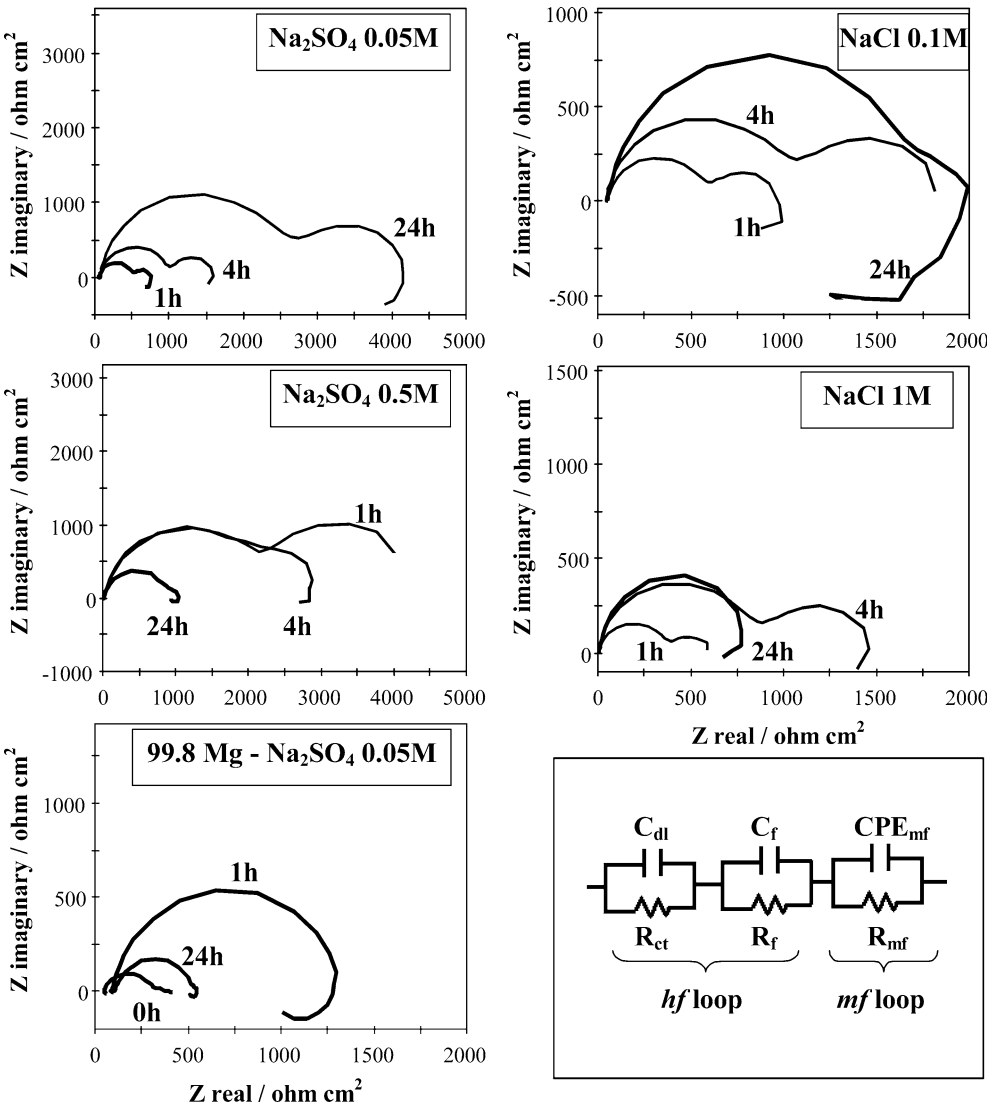

Fig. 9. Impedance spectra recorded in dilute or concentrated Na_2SO_4 or NaCl solutions at various immersion times.

shorter time interval from 10 to 30 Ω cm^2 and successively they decreased, attaining, after 24 h, a value close to 5–10 Ω cm^2. By continuing the test, R_{CT} augmented again, slightly in chlorides and more markedly in sulphates. At the end of the test, the value in sulphates was markedly higher than that in chlorides (30 and 10 Ω cm^2, respectively).

The evolution of R_F showed that the surface film formed at the same velocity in both dilute environments: R_F increased during the first day and was almost constant, but the film formed in sulphates was a little more protective (R_F around 2.2 kΩ cm^2) than that in chlorides (R_F around 1.6 kΩ cm^2) (Figure 10). In the concentrated media the trends markedly differentiated from each other. Initially, in chlorides, the evolution of R_F was equal to that in diluted solution, but, after 8–12 h, it attained its maximum values (950 Ω cm^2). Subsequently, a slow drift to lower values was experienced (R_F = 450 Ω cm^2, at 96 h). In sulphates, the protective layer tended to form more rapidly: R_F reached a value over 2 kΩ cm^2 after only 2 h of immersion. In the following 6 h, it decreased rapidly down to about 1 kΩ cm^2 and successively it presented the same drift found in chlorides.

In the dilute solutions, C_F values of WE43 diminished at the beginning of the immersion, and then remained almost constant. In sulphates C_F was initially higher than that in chlorides (23 and 15 μF cm^{-2}, respectively), but, at the end of the test, the film capacitances were equal (Table 2). In concentrated chloride solutions, C_F displayed some fluctuations around an average value, very close to the initial value measured in the diluted solution. In concentrated sulphate solution, on immersion, the value of C_F was much lower than that in the diluted solution. It presented a small decrease in the first hour of immersion, but, successively, tended to increase.

The second capacitive loop, associated with diffusion phenomena through the corrosion product layer, was observed just after the immersion, although it was very small. This means that the formation of the multilayered film is nearly instantaneous.

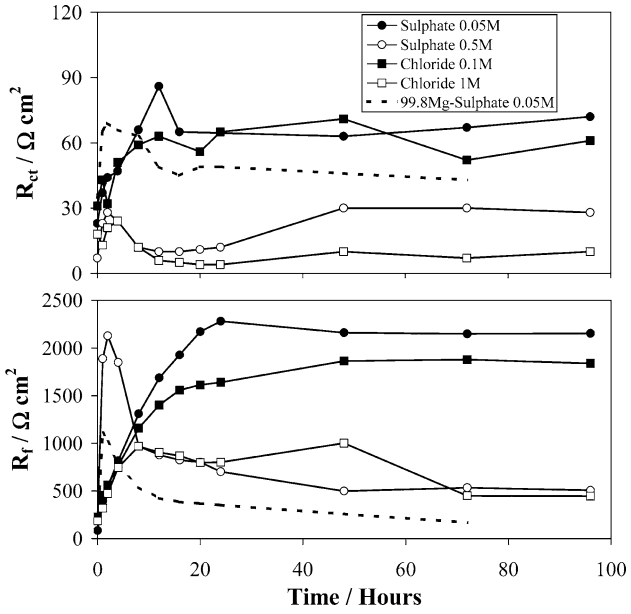

Fig. 10. Trend of charge transfer resistance (R_{CT}) and passive film resistance (R_F) in Na_2SO_4 or NaCl solutions.

The *mf* semicircle was simply modelled by a Constant Phase Element (CPE)-Resistance parallel network. The trends of the CPE_{mf}, *n* exponent and R_{mf} parameters are reported in Figure 11.

In 0.05 M sulphate solution R_{mf} increased in few hours from around 30 to 1600 Ω cm^2, then it attained an almost constant value; at the same time CPE_{mf} value reduced from 5 to 1.5 μF cm^{-2}; *n* exponent value remained close to 0.9. In 0.5 M solution, initially R_{mf} increased very rapidly during the early stages of immersion from about 100 to 1500 Ω cm^2 and CPE_{mf} diminished from around 6 to 0.5 μF cm^{-2}. Then a decay in R_{mf} and fluctuations in CPE_{mf} were observed. Only in this case, did *n* exponent remain close to the value of 0.5, indicating a purely diffusive nature of this capacitive loop.

The evolution of R_{mf}, CPE_{mf} and *n* exponent in diluted chloride solution was similar to that in the corresponding sulphate solution. In concentrated chloride media R_{mf} initially increased as in the diluted one, and CPE_{mf} diminished, while *n* exponent was close to 0.8. However, the sudden disappearance, after about 8 h, of the *mf* loop could be related to heavy damage in the protective surface film induced by chlorides.

Figure 9 also presents some impedance spectra of 99.8 Mg alloy in the dilute sulphate solution. At the beginning of the immersion, these spectra presented either the *hf* and *mf* responses of RE containing alloy, but, successively, the *mf* loop tended to be heavily reduced or to disappear.

For 99.8 Mg alloy, R_{CT} and R_F values sharply increased in the first hours of immersion (Figure 11), then they, more or less slowly, decreased. This trend was particularly evident for the film resistance. R_{CT} and R_F values of 99.8 Mg specimen, after a short time, were lower than those of WE43 specimen. While the differences in R_{CT} between the two alloys were negligible, the differences in R_F were noticeable: R_F of WE43 was over 2 kΩ cm^2 and of 99.8 Mg was less than 0.5 kΩ cm^2, in agreement with the four-fold higher corrosion rate values measured on this alloy than that measured on WE43 alloy.

During the whole test, C_F values of 99.8 Mg were always lower than those of the RE containing alloy.

4. Discussion and conclusions

It is well known that, during magnesium alloy corrosion, a protective layer of oxide and hydroxide is formed on the metal surface [9], whose performances depend on the electrolyte type [3]: an extremely protective behaviour is induced by strongly passivating anions, such as chromates or fluorides, while negative effects are produced by pitting agents, such as chlorides. In this context, sulphates are reputed to moderately stimulate corrosion. Weight loss data and polarization curves of WE43 alloy show the usual high tendency of chlorides to damage or destroy the protective passive film. At the same time, the wider potential interval of high slope and the current decrease as a function of time in the anodic polarization curves evidence the higher propensity of sulphates, as compared to chlorides, to the formation or maintenance of this protective film. The comparison between V_{DISS} of WE43 alloy and 99.8 Mg and the anodic polarization curves sustain the improvement in magnesium capability to passivate, afforded by RE elements.

EIS measurements can give further information about the influence of these elements on the corrosion behaviour of magnesium alloys. The similar values and time evolution of R_{CT} between WE43 and 99.8 Mg alloys (or

Table 2. Values of C_F (μF cm^{-2}) as a function of time

Specimen	Electrolyte	Conc./M	Time/h						
			0	1	2	4	12	24	96
WE43	Sulphates	0.05	23	19	17	15	15	15	14
		0.5	11	8	8	9	12	12	11
	Chlorides	0.1	15	13	12	12	12	12	14
		1	16	14	16	15	14	17	14
99.8 Mg	Sulphates	0.05	18	10	10	11	12	13	18*

*After 72 h immersion.

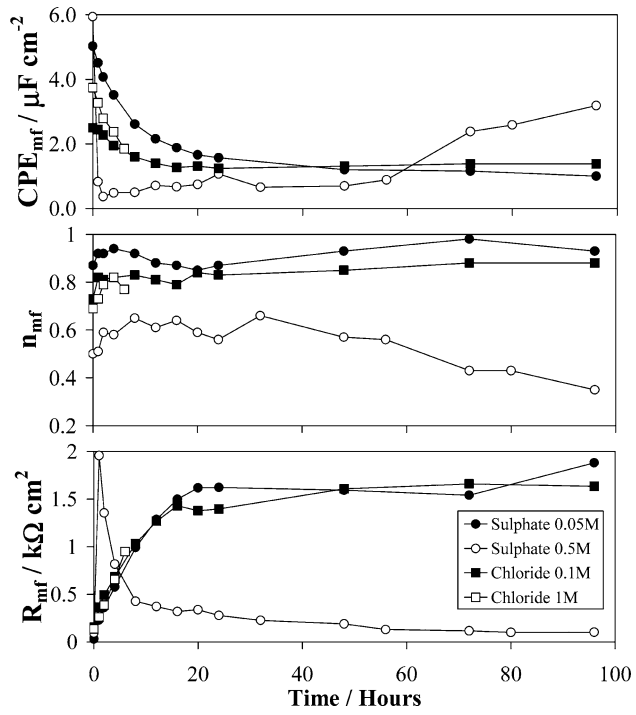

Fig. 11. Trends of CPE, *n* exponent and resistance related to the second capacitive loop (R_{mf}) in dilute and concentrated Na_2SO_4 or NaCl solutions.

pure Mg [7]) show that the magnesium charge transfer process is not strongly influenced by the alloyed RE elements. At low concentrations, sulphates and chlorides present about the same charge transfer resistance, which increases by elapsing the immersion time. In concentrated solutions, R_{CT} is smaller than that in diluted ones because both electrolytes favour the anodic oxidation of magnesium. R_{CT} initially increases, but then diminishes with the testing time: it can be assumed that this is due to a corroded area enlargement as a result of flaw accumulation in the passivating layer.

However, R_F parameter, inversely proportional to corrosion rate, shows that RE elements improved the protective performances of the film passive. In diluted media such a film forms with the same rate both in chlorides and in sulphates. In concentrated solutions, the layer forms very quickly in the presence of sulphates; then it is damaged by the action of the anions and after very few hours its protective effects are markedly reduced. In the case of chlorides these effects are almost completely annulled.

R_F values for WE43 are greater than those corresponding to 99.8 Mg and pure Mg and similar to those of AZ91 alloy [8], but they increase more rapidly than those of the latter alloy, attaining a superior final value. This accounts for the formation of a more protective film in the RE containing specimen.

Furthermore, the higher R_{mf} values of WE43, as compared to those of AZ91 [8] show that the diffusion process through the film of corrosion products on WE43 is more strongly hindered. In the case of 99.8 Mg alloy, the lack of an evident and large *mf* capacitive loop can be a further indication that its corrosion product layer is scarcely protective and does not exert a clear limitation to the diffusion stage of the corrosion process.

It is likely that the RE elements increase the resistance to the Mg^{2+} cation egress through MgO layer [23] and retard its hydration process, thus improving the passivating characteristics of the corrosion product layer [24]. To this purpose, it was recently found that the presence of Nd rendered the dissolution of Mg_{82}–Ni_{18} amorphous alloys less severe [26] by decreasing the tendency of MgO to turn into $Mg(OH)_2$.

The film capacitance values can give a qualitative indication of the evolution of the layer thickness, particularly in the less aggressive sulphate solutions: C_F should decrease as a result of a thickening of the layer and increase due to an enlargement of the corroded surface. In dilute media, the time trend of C_F for WE43 alloy (C_F = 23 μF cm^{-2}, t = 0; C_F = 13 μF cm^{-2}, t = 16 h) shows that this layer almost doubles its thickness during the initial 16 h of immersion, while the corresponding R_F has a 20-fold increase; in concentrated media, its thickness is higher than the previous ones, due to a stronger corrosion attack. The thickness rapidly augments but the successive C_F increase points to a film damage phenomenon and to a widening of the corroded area. These high C_F values, of the order of 10 μF cm^{-2}, i.e. close to the usual C_{DL} values, are attributed to a non perfect, porous layer [3].

C_F of WE43 alloy is higher than that of 99.8 Mg (and that of pure Mg too[7]) and this may be linked to a thinner surface film, which, however, considering the film resistance values, is more protective. At the beginning of the test, for both alloys, film thickening takes place. Successively, an enlargement in the corroded area prevails for 99.8 Mg, whereas for RE containing alloys a steady-state condition between film thickening and corroded area increase occurs.

In the dilute solutions, where undermining effects are less severe and the corrosive attack can be considered mainly generalized, LPR and EIS measurements sustain weight-loss data. In this case R_F can give an indication of the corrosion resistance of the alloy.

In the concentrated solutions, particularly in the case of chlorides, where severe grain disbonding may occur, some justified differences can be found between gravimetric and electrochemical measurements at long immersion times. However, EIS measurements evidence the diminution of the protective performances of the passive layer (i.e. diminution in R_F and R_{mf}).

Acknowledgement

This work was financially supported by Local University Funds.

References

1. T.J. Polmear, *Light Alloys*, 3rd ed., (Arnold, London, U.K., 1995).
2. J.F. Nie, in H.I. Kaplan (Eds), *Magnesium Technology 2002* (The Institute of Metals, London, 2002), pp. 103–110.
3. E. Gulbrandsen, *Electrochim. Acta* **37** (1992) 1403.
4. E. Guldbransen, J. Tafto and A. Olsen, *Corros. Sci.* **34** (1993) 1423.
5. N. Pébère, C. Riera and F. Dabosi, *Electrochim. Acta* **35** (1990) 555.
6. F. Dabosi, R. Morancho, N. Pébère and D. Pouteau, in *Proceedings 47th Annual World Magnesium Conference* (The International Magnesium Association, Cannes, France, 1990), pp. 51–55.
7. G. Baril and N. Pébère, *Corros. Sci.* **43** (2001) 471.
8. G. Baril, C. Blanc and N. Pébère, *J. Electrochem. Soc.* **148**(12) (2001) B489.
9. G. Song and A. Atrens, *Adv. Eng. Mat.* **1** (1999) 11.
10. G. Song, A. Atrens, D. StJohn, J. Nairn and Y. Li, *Corros. Sci.* **39** (1997) 855.
11. G. Song, A. Atrens, D. StJohn, X. Wu and J. Nairn, *Corros. Sci.* **39** (1997) 1981.
12. G. Song, A. Atrens, X. Wu, Z. Bo and B. Zhang, *Corros. Sci.* **40** (1998) 1769.
13. G. Song, A. Atrens and M. Dargush, *Corros. Sci.* **41** (1999) 249.
14. G. Song, *J. Corros. Sci. Eng.* **6** (2003) paper C104.
15. W. Unsworth and J.F. King, *Magnesium Technology* (The Institute of Metals, London, 1987), p. 25.
16. B. Geary, in *Proceedings ASM International Conference on Advanced Aluminium and Magnesium Alloys* (Amsterdam, 20–22 June, ASM Europe, Brussels, 1990), pp. 773–780.
17. I. Nakastugawa, S. Kamado, Y. Kojima, R. Ninomiya and K. Kubota, *Corros. Rev.* **16** (1998) 139.
18. J.I. Skar and D. Albright, in H.I. Kaplan (Ed.) *Magnesium Technology 2002* (The Institute of Metals, London, 2002), pp. 255–261.
19. K. Nişancioğlu and J.H. Nordlien, *J. Jpn. Inst. Light Metals* **50**(9) (2000) 417.
20. G. Song and D. StJohn, *J. Light Metals* **2** (2002) 1.
21. J.H. Nordlien, S. Ono, N. Masuko and K. Nişancioğlu, *J. Electrochem. Soc.* **142** (1995) 3320.
22. J.H. Nordlien, K. Nişancioğlu, S. Ono and N. Masuko, *J. Electrochem. Soc.* **143** (1996) 2564.
23. J.H. Nordlien, S. Ono, N. Masuko and K. Nişancioğlu, *J. Electrochem. Soc.* **144** (1997) 461.
24. J.H. Nordlien, S. Ono, N. Masuko and K. Nişancioğlu, *Corros. Science* **39** (1997) 1397.
25. G. Baril, C. Blank and N. Pébère, *Electrochem. Soc. Proc.* **23** (2000) 166.
26. H.B. Yao, Y. Li, A.T.S. Wee, J.S. Pan and J.W. Chai, *Appl. Surf. Sci.* **173** (2001) 54.